Accident Analysis and Prevention 82 (2015) 244–256

Contents lists available at ScienceDirect

Accident Analysis and Prevention

journal homepage: www.elsevier.com/locate/aap

Development and evaluation of a finite element model of the THOR for occupant protection of spaceflight crewmembers

Jacob B. Putnam[a], Jeffrey T. Somers[b], Jessica A. Wells[c], Chris E. Perry[d], Costin D. Untaroiu[a,*]

[a] Center for Injury Biomechanics, Department of Biomedical Engineering and Mechanics, Virginia Tech, Blacksburg, VA, USA
[b] Wyle Science, Technology and Engineering Group, Houston, TX, USA
[c] Lockheed Martin, Houston, TX, USA
[d] 711th Human Performance Wing, Wright-Patterson Air Force Base, OH, USA

ARTICLE INFO

Article history:
Received 13 July 2014
Received in revised form 2 May 2015
Accepted 4 May 2015
Available online 20 June 2015

Keywords:
Crash test dummy
Impact biomechanics
Human-volunteer testing
Biofidelity
Anthropomorphic test device
Human spaceflight

ABSTRACT

New vehicles are currently being developed to transport humans to space. During the landing phases, crewmembers may be exposed to spinal and frontal loading. To reduce the risk of injuries during these common impact scenarios, the National Aeronautics and Space Administration (NASA) is developing new safety standards for spaceflight. The Test Device for Human Occupant Restraint (THOR) advanced multi-directional anthropomorphic test device (ATD), with the National Highway Traffic Safety Administration modification kit, has been chosen to evaluate occupant spacecraft safety because of its improved biofidelity.

NASA tested the THOR ATD at Wright-Patterson Air Force Base (WPAFB) in various impact configurations, including frontal and spinal loading. A computational finite element model (FEM) of the THOR to match these latest modifications was developed in LS-DYNA software. The main goal of this study was to calibrate and validate the THOR FEM for use in future spacecraft safety studies.

An optimization-based method was developed to calibrate the material models of the lumbar joints and pelvic flesh. Compression test data were used to calibrate the quasi-static material properties of the pelvic flesh, while whole body THOR ATD kinematic and kinetic responses under spinal and frontal loading conditions were used for dynamic calibration. The performance of the calibrated THOR FEM was evaluated by simulating separate THOR ATD tests with different crash pulses along both spinal and frontal directions. The model response was compared with test data by calculating its correlation score using the CORrelation and Analysis rating system. The biofidelity of the THOR FEM was then evaluated against tests recorded on human volunteers under 3 different frontal and spinal impact pulses.

The calibrated THOR FEM responded with high similarity to the THOR ATD in all validation tests. The THOR FEM showed good biofidelity relative to human-volunteer data under spinal loading, but limited biofidelity under frontal loading. This may suggest a need for further improvements in both the THOR ATD and FEM. Overall, results presented in this study provide confidence in the THOR FEM for use in predicting THOR ATD responses for conditions, such as those observed in spacecraft landing, and for use in evaluating THOR ATD biofidelity.

1. Introduction

With the advent of new space-crew-transport vehicles being developed by the National Aeronautics and Space Administration (NASA) and several commercial companies, the number of spaceflight occupants is expected to increase dramatically. Learning from the trials of the automotive safety field, early development of occupant crash safety standards for these new spaceflight vehicles will be essential in the prevention of injury and preservation of human life. Though the necessity of standards can be learned from the automotive field, the spaceflight standards need to be developed separately due to vast differences between these fields. An automobile impact is a low-occurrence, high-risk event with a crash impact risk of 1 in 1.3 million miles driven and 1 in 3.4 crashes resulting in injury (NHTSA, 2014). Therefore,

* Corresponding author at: Virginia Tech, Department of Biomedical Engineering and Mechanics, Center for Injury Biomechanics, VCOM II Building, 2280 Kraft Drive, Blacksburg, VA 24060, USA. Tel.: +1 540 231 8997; fax: +1 540 231 2953.
E-mail addresses: costin@vt.edu, costin.untaroiu@gmail.com (C.D. Untaroiu).

http://dx.doi.org/10.1016/j.aap.2015.05.002
0001-4575/

automobile industry standards are focused on mitigating the risk of severe injuries. To achieve spaceflight, the human body is accelerated to over 11,200 m/s to escape Earth's gravity and in turn is decelerated back to 0 m/s during landing (Newby et al., 2013). Though peak accelerations are reduced as much as possible, there is still a large energy transfer into the body during takeoff and landing. Therefore, it is essential to develop spaceflight safety standards with a very conservative total injury risk to ensure the continued health and safety of all human occupants traveling to and from space.

The space-crew-transport vehicles currently being developed for NASA are the Orion, SpaceX Dragon, and Boeing CST-100. All are capsule based and each has a unique landing acceleration environment based on the individual designs (Newby et al., 2013). The Sierra Nevada Corporation Dream Chaser lifting-body space-transport vehicle is not currently under consideration by NASA (Foust 2014; Somers et al., 2014a); however, these designs may be used for commercial space transportation outside of NASA. During takeoff, the crewmembers experience posterior–anterior accelerations. During landing, crewmembers typically experience accelerations in inferior–superior (spinal) and either anterior–posterior (frontal) or posterior–anterior (rear) directions. Though nominal takeoff conditions can be highly controlled, launch aborts may impart a large load on the crewmembers and may include significant off-axis oscillatory accelerations. Capsule landing is usually controlled by parachutes, thus dependent on wind conditions and parachute performance. In addition, wave slope and direction or ground terrain can also greatly influence the landing loads. The variability in landing conditions further adds to the necessity of conservative injury risk standards, requiring thorough crash safety analysis of these conditions.

Crash safety analysis is primarily performed through the testing of anthropometric test devices (ATDs), commonly referred to as crash test dummies. Currently, NASA is investigating the Test Device for Human Occupant Restraint (THOR) ATD for use in the development of new spaceflight safety standards. The THOR ATD, developed by the National Highway Traffic Safety Administration (NHTSA), was chosen for this investigation due to its improved biofidelity over other common ATDs, specifically the industry standard Hybrid III ATD (Shaw et al., 2002).

NASA performed a series of frontal and spinal impact tests on the THOR ATD at the Wright-Patterson Air Force Base (WPAFB) to assess responses in spaceflight-like landing conditions (Newby et al., 2013). The purpose of the testing was twofold: to understand the physical response of the THOR ATD to conditions similar to expected spaceflight impacts, and to provide test data for model calibration and validation. The acceleration pulses were sinusoidal, ranging from 10 to 20-*g* at a 70 ms rise time. In addition, 10-*g* runs were conducted with 40 and 100 ms rise times to assess the frequency response of the THOR ATD. Although these pulses are not the exact anticipated loads for the NASA Orion vehicle, they were selected to cover the range of accelerations and rise-times expected during nominal and off-nominal landing conditions. A subset of these test data was used to calibrate and validate the THOR FEM in frontal and spinal loading.

The increase in computational power over the last decade has enabled the use of a computational component complementary to experimental testing. The development of a finite element model (FEM) in the crash safety field presents many opportunities to increase the efficiency and capabilities of human safety analysis. An accurate and reliable THOR FEM provides a tool to increase testing efficiency, as simulated test setups can easily be adjusted to assess response in a variety of conditions. In addition, these models allow for the optimization of vehicle or restraint system design throughout the manufacturer's design process (Untaroiu et al., 2007; Bose et al., 2010; Adam and Untaroiu, 2011).

The goal of this study was to develop an accurate THOR FEM for spaceflight crash safety analysis. The effectiveness of the THOR FEM was ensured through comparison to physical tests in both frontal and spinal impacts. Once verified against the THOR ATD, the THOR FEM was used to assess biofidelity against human-volunteer test data. Based on these results, recommendations are made on the effectiveness of the THOR to predict human response in the spaceflight loading regimen. The THOR FEM may be used to aid in the development of new spaceflight occupant safety standards, provide an effective tool in the optimization of new vehicle designs without the expense of testing and physical prototyping, and continually improve the THOR ATD biofidelity.

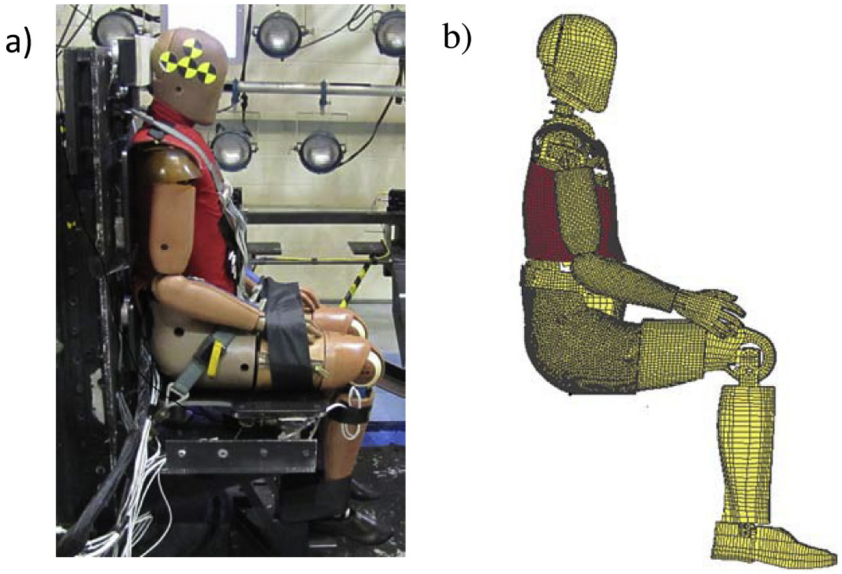

Fig. 1. THOR: (a) ATD, (b) FEM.

2. Methods

2.1. Development and updating of the THOR FEM

The THOR FEM (Untaroiu et al., 2009) was updated according to recent modifications made to the THOR ATD to improve its durability, usability, and biofidelity (Ridella and Parent, 2011). A schematic of the ATD and its FEM can be seen in Fig. 1. The FEM of updated ATD regions were developed (Putnam et al., 2014) based on CAD drawings using HyperMesh software (Altair Engineering, Inc., Troy, MI, USA). The updated model components were calibrated and validated against component certification test data (Yue et al., 2013; Putnam et al., 2014), and then were assembled into the complete THOR FEM in LS-DYNA (Livermore Software Technology Corporation, Livermore, CA, USA), which contains 222,292 nodes and 444,324 elements, and allows simulations with a time step of 0.65 μs. A positioning tree of the THOR FEM was developed in LS-PrePost (Livermore Software Technology Corporation, Livermore, CA, USA) to allow proper adjustment of the model posture to various test setups. The posture ranges were constrained to the positioning capabilities of physical ATD. Load cells and accelerometer models were also implemented within the FEM to match the physical ATD instrumentation.

2.2. Model calibration

Material data for the updated THOR ATD were not publicly available therefore to improve the response of the THOR FEM for typical spaceflight takeoff and landing impact conditions (frontal and spinal directions), material parameters of parts deemed essential to responses in these conditions were calibrated from the baseline values assigned in the previous THOR FEM (Untaroiu et al., 2009). It has been previously shown (Putnam et al., 2013, 2015) that the overall response of the previous THOR FEM in spinal loading is significantly influenced by the properties assigned to the pelvic flesh. In addition, the rubber flex joints in the spinal column were shown to have a significant effect on the FEM response in both impact directions during several preliminary simulations. Therefore the upper-thoracic flex joint (UFJ), lower-thoracic flex joint (LFJ), and pelvic flesh were chosen to be calibrated. The static and dynamic stiffness curves of the pelvic-flesh-material model (LS-DYNA Material Model 83, MAT_FU_CHANG_FOAM (LS-DYNA, 2007)) and the flex-joint-material models (LS-DYNA Material Model 183 MAT_SIMPLIFIED_RUBBER_WITH_DAMAGE (LS-DYNA, 2007)) were calibrated to optimize response to available ATD test data (Fig. 2). The robustness of this calibration was verified with 2 independent-model-validation-test cases unique from the test cases used for model calibration.

2.2.1. Calibration of pelvic flesh under quasi-static loading

The quasi-static stress–strain curve defined in the THOR FEM pelvic-flesh material was calibrated to match the force data recorded in a quasi-static-compression test (Mike Beebe, 2010). The test setup consisted of the pelvic flesh fitted onto a rigid metallic substructure (Fig. 3). A flat plate compressed the bottom of the pelvic flesh to 30 mm and then uncompressed it at a constant rate of 250 mm/min. This setup was simulated by constraining the interior nodes of the pelvic-flesh model to a fixed rigid part. A flat shell plate was then simulated to compress the pelvic flesh as done in testing.

Using this simulation, the scale factor of the quasi-static strain–stress curve was determined by attempting to match the force–displacement time history between the pelvic flesh and rigid plate, in an optimization process carried out in LS-OPT version 4.0 (Livermore Software Technology Corporation, Livermore, CA). A successive-response-surface methodology (SRSM) with linear approximation was used with the objective function set to curve mapping between simulation and test data. The pelvic stiffness-scale factor was the

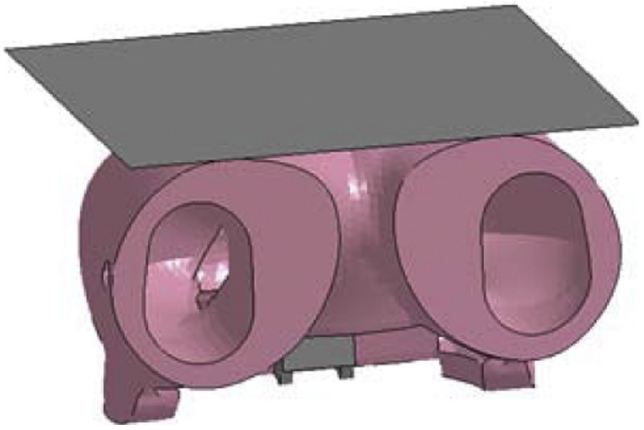

Fig. 3. Pelvis flesh quasi-static compression setup: FEM simulation.

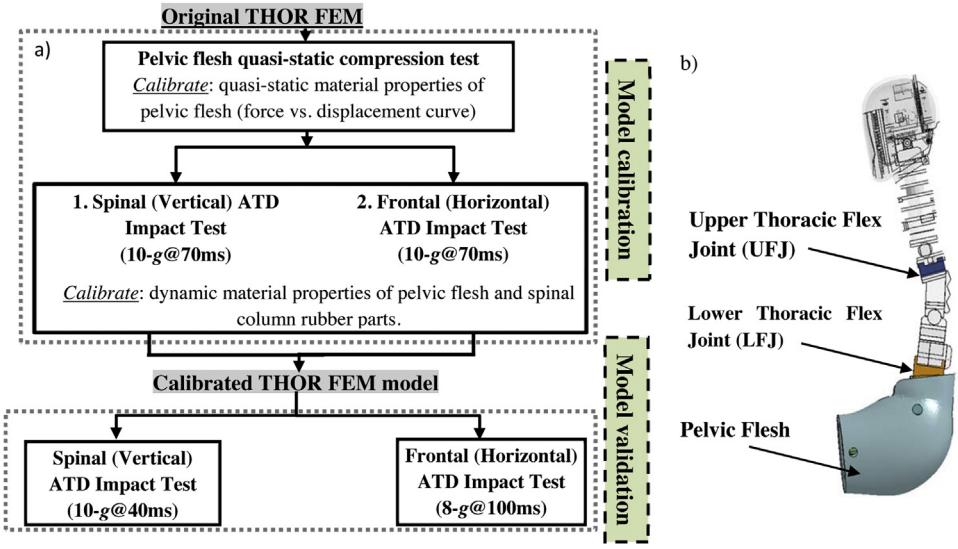

Fig. 2. (a) Schematic of the calibration and validation of the THOR FEM with (b) diagram of calibrated parts.

only defined variable and was varied between 0.50 and 0.010, based on the results of several preliminary simulations. Two iterations with a total of 40 simulations were run with an explicit solver in multi-parallel processing (MPP) on the Argonne National Labs' Transportation Research and Analysis Computing Center (TRACC). The total run time per simulation was approximately 10 h with 8 CPU per run.

2.2.2. Calibration of the THOR FEM under spinal and frontal loading

A THOR ATD with all the modification kit upgrades excluding the SD-3 shoulder and a generic test seat with rigid back and seat pan were used in testing (Ridella and Parent, 2011). A small layer of felt padding was placed over the head plate. The ATD was restrained to the seat with a 5-point belt system consisting of a double shoulder strap, lap belt, and negative-*g* strap, each pre-tensioned to (89 ± 22 N) (Fig. 4a). In addition the ATD hands and feet were attached to the legs and chair respectively to prevent excessive flailing. Acceleration conditions were driven by the horizontal impulse accelerator (HIA) which demonstrated a uniform 5% reproducibility on peak acceleration and velocity profile (Strzelecki, 2005). Data were collected from the THOR ATD instrumentation at 10,000 samples per second using a 3 kHz anti-aliasing 5-pole filter (Newby et al., 2013).

A seat model was developed based on the test-seat dimensions recorded using a FAROArm coordinate measuring machine (FARO Technologies, Conventry, UK). The THOR FEM was positioned within the seat model with appropriate contacts defined between the seat and restraint models and the THOR FEM (Fig. 4b). A pretest initialization simulation was performed during which gravitational acceleration was applied to the THOR FEM until a steady state of compression against the fixed seat was reached. The final nodal positions of the compressed parts were saved and used to define the FEM's initial position. The difference in nodal position of compressed parts was used to define the initial stress state of the model. The ATD was positioned upright to gravity in the frontal test and lying on its back in the spinal test, and pre-simulation initialization was performed accordingly for each test condition. The material properties of the restraint system used in testing were determined through quasi-static-tensile tests of each belt part. Then, a material model (LS-DYNA Material Model B01, MAT_SEATBELT (LS-DYNA, 2007)) was used to assign the determined material properties to each belt-model part (Fig. 4b and c). A second pretest simulation was run to pretension the belt around the THOR FEM to 89 N. In addition, spring models were used to restrain the hands and feet of the THOR FEM as in testing.

The calibration of the entire THOR FEM was performed using test data recorded in 1 spinal and 1 frontal impact condition, both with nominal 10-*g* peak acceleration and 70 ms rise time. Acceleration pulses measured during testing were applied to the seat model. Acceleration pulses were applied to the model along the spinal (inferior–superior) (Fig. 5a) and the frontal (anterior–posterior) directions (Fig. 5b). The seat model was constrained in all other directions. Baseline simulations were first run over the full pulse length in both testing directions to determine the minimal run time necessary to encompass peak response in all analyzed signals. It was found that 100 ms in the spinal simulation and 150 ms in the frontal direction satisfy this requirement. Therefore, these values were used as the run times for the spinal and frontal calibrations, which required a large number of simulations, to increase their time efficiency.

2.2.3. Model correlation rating

The overall response of the THOR FEM was quantitatively rated against test data to provide an objective metric for model calibration. The quality of a model's response in safety application has traditionally been evaluated by comparing peak values to test data, qualitative analysis of curve shape, and/or through defined certification criteria. None of these techniques provide a quantitative means for grading the total response of a model based off the entire time history of its response. Recently there has been a focus to develop new curve-to-curve analysis techniques (Jacob et al., 2000; Sarin et al., 2008; Gehre et al., 2009; Pellettiere and Moorcroft, 2012; Untaroiu et al., 2013). From these efforts, the CORrelation and Analysis (CORA) signal rating software was developed (Thunert, 2012). The CORA rating method is made up of two independent-rating methods, a corridor rating and a cross-correlation rating (Fig. 6). The corridor method scores the simulation curve based on its position within inner and outer corridors developed around the test curve. Each evaluated curve is split into finite intervals which are individually scored and averaged. A score of 1 is given if the simulation is within the inner corridor, a score of 0 is given outside of the outer corridor, and a score between 0 and 1 is calculated by interpolation for the region between inner and outer corridors.

The interval scores are averaged to calculate the total corridor score (S_{co}). The cross-correlation method rates the simulation curve, between 1 (perfect match) and 0 (no correlation) based on 3 characteristics with respect to the test curve (Fig. 6). Phase-shift score (S_{ps}), progression score (S_p) and size score (S_s) are measures of curve position, curve shape, and peak value, respectively (Fig. 6) (Thunert, 2012). The value of CORA scores are highly influenced by the global setting parameters used in calculation (e.g., the parameters to define the inner/outer corridor). To be consistent, the same parameter set recommended in the latest CORA manual (Thunert, 2012) was used in all rating evaluations.

The CORA rating of a curve (signal) is calculated as a linear combination of the corridor and the cross-correlation scores:

$$S_{cora} = w_{co}S_{co} + w_{cc}S_{cc} \quad (1)$$

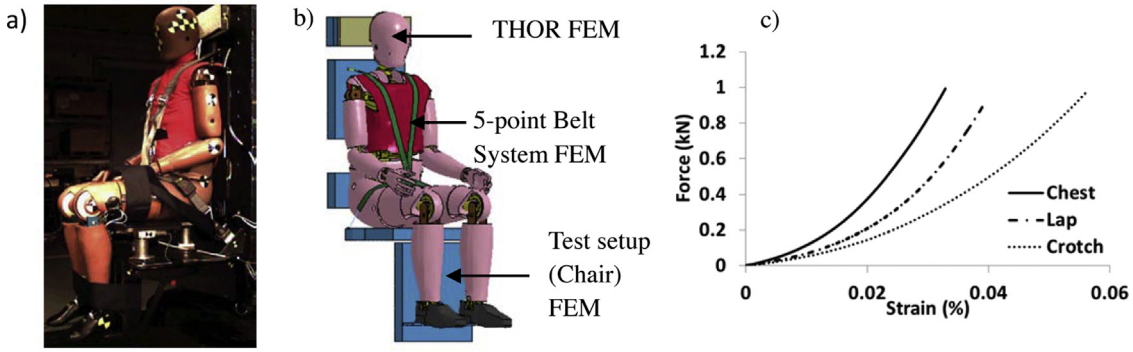

Fig. 4. THOR test setup: (a) ATD, (b) FEM, (c) belt stiffness curves.

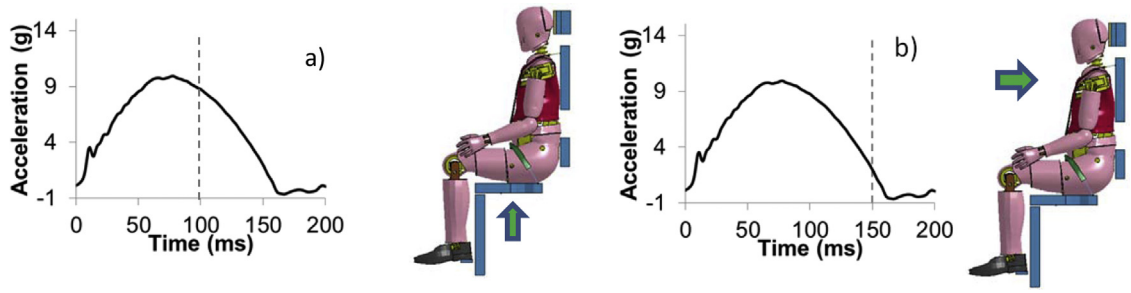

Fig. 5. Model calibration: acceleration pulses used in the THOR FEM simulations. (a) Spinal (vertical) direction, (b) frontal (horizontal) direction.

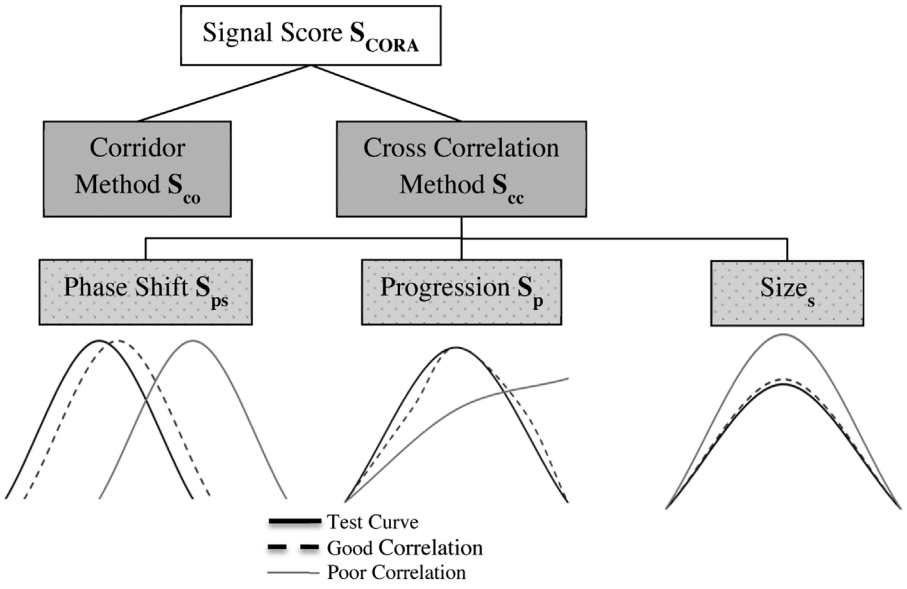

Fig. 6. Schematic of CORA rating methodology.

the cross correlation score is calculated:

$$S_{cc} = w_{ps}S_{ps} + w_pS_p + w_sS_s \quad (2)$$

The values of weighting factors were evenly set: $w_{co} = w_{cc} = 1/2$, and $w_{ps} = w_p = w_s = 1/3$.

The CORA-model rating, defined as the average of all signals evaluated, was used to provide an objective model score for the dynamic-material-model calibration. To perform the model calibration, both frontal and spinal simulations were run in LS-DYNA within the same optimization process, with model material parameters iteratively selected using a design of experiments scheme and SRSM with elliptic approximation optimization algorithm implemented in LS-OPT (Livermore Software Technology Corporation, Livermore, CA, USA) (Fig. 7). Model response signals were chosen for CORA comparison based on relevance to typical injury criteria for the given impact direction and to encompass the entire ATD response. Both ATD and FEM response data were filtered using a channel frequency class (CFC) 180 4-pole phaseless digital filter complying with the Society of Automotive Engineers recommended practices for impact test electronic instrumentation, SAE J211 (SAE, 1995). The average CORA model rating for both directions was set as the objective function that was maximized during the optimization process. The optimization algorithm and all simulations were run on the TRACC cluster using an explicit solver in MPP with 8 CPU per run with an approximate run time of 6 h per simulation. There were 128 simulations run in both test directions over 4 iterations.

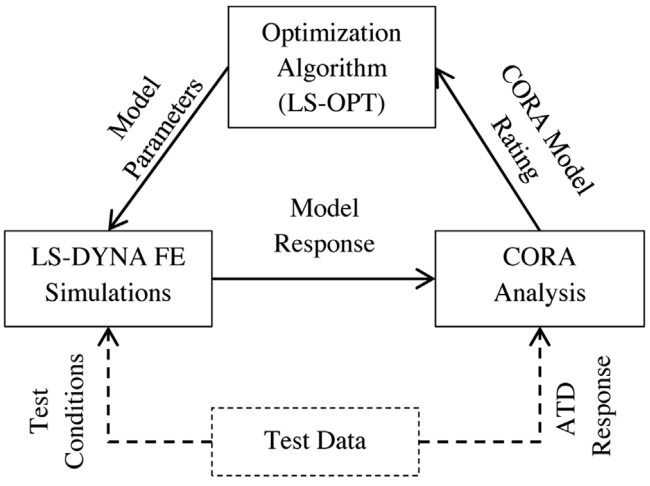

Fig. 7. Schematic of the calibration method.

To calibrate the dynamic stress–strain properties of the pelvic flesh, each rate dependent stress–strain curve defined in the pelvic flesh material model was scaled individually (LS-DYNA, 2007) (Fig. 8a). To prevent the curves from overlapping, the scale factor of each curve was calculated by the formula: $SF_n = SF_{n-1} + X_n$ (where SF is the scale factor, X is the optimization variable, and n represents each strain rate). SF_0 was assigned as the quasi-static-scale factor previously determined. X_n was calibrated over a range of 0–0.5. The unloading properties of the pelvic flesh were

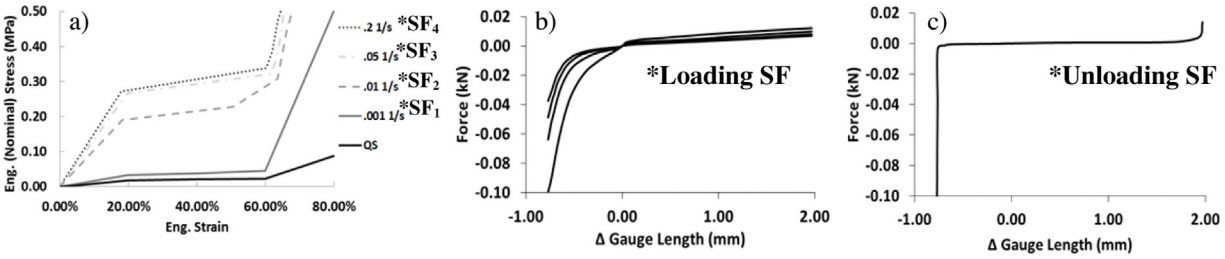

Fig. 8. (a) Stress–strain curves of pelvis flesh model. Force–displacement curves of spinal column rubber: (b) loading and (c) unloading.

calibrated by adjusting the hysteretic unloading factor (HU) and shape parameter (SH) defined in the material model. The HU was varied between 0.1 and 0.9 while SH was varied between -1 and 6. The force–displacement curves of the UFJ and LFJ were scaled in both loading and unloading (Fig. 8b and c) between 0.1 and 10. The ranges of variables were defined based on the results of our preliminary simulations. To simplify the total number of parameters used in optimization all loading rate curves for the UFJ and LFJ parts were scaled using a single scale factor. All 10 variable ranges used in optimization were chosen based on pretest simulations.

2.3. Model validation

The calibrated THOR FEM was simulated under different spinal/frontal impact pulses to ensure calibration improvements were not test specific. Acceleration pulses of 10-*g* with 40 ms rise time and 8-*g* with 100 ms rise time were used respectively for the spinal and frontal validation simulations (Fig. 9a and b). The same response signals used during the calibration phase were evaluated using the CORA-rating system in the validation phase.

2.4. Comparison of dummy-to-human responses under spinal and frontal impact loadings

The THOR FEM, validated under frontal and spinal loading conditions, was used to evaluate the biofidelity of the FEM against historical human-volunteer-test data performed at WPAFB. The model response at nominal impact accelerations of 6, 8, and 10-*g* in both frontal and spinal test directions was compared to human male volunteer data recorded in a frontal impact test series (Study #200301) and a spinal impact test series (Study #199906) (Buhrman 1998; Cheng and Buhrman, 2000). Although the dataset contained both male and female subjects, the comparison was limited to only the unscaled data recorded in male subjects, as the THOR is a representation of a 50th percentile male. The number of WPAFB volunteer tests performed with each impact pulse and the age/anthropometric data of male subjects are reported in Table 1.

The human-volunteer-frontal-impact study was performed on the WPAFB HIA similar to the THOR tests (Fig. 10a). The chair model used in calibration and validation (Fig. 4b) was adjusted to the dimensions of the 40-*g* seat fixture used in this test. The back plate was extended, a foot plate was added, and then the THOR FEM was positioned to match the human test conditions. A generic HGU helmet model was developed to approximate the geometry and inertial properties (mass, center of gravity, and moment of inertia) of the helmet used in testing. An oxygen mask was additionally modeled to represent the equipment worn by human subjects. The previously developed 5-point belt model was fit to the new seat model and pretensioned to 89 N according to the test setup.

The human-volunteer-spinal-impact study was performed on the WPAFB vertical deceleration tower (VDT) (Fig. 10b). The THOR FEM was positioned into a generic seat model as in testing. This study used a similar belt setup to the HIA tests, with the exception of the negative-*g* strap, which was removed from the model. In both frontal and spinal tests, the subject's head acceleration was measured within a bite block and chest acceleration was measured using Velcro™ strapped accelerometers on the subject's chest center. In the FEM, chest acceleration was calculated at the mid-sternal accelerometer location and the head acceleration was calculated at a point defined on the head casting approximate of the posterior jaw. Due to increased noise in the human data set in comparison to the FEM tests, both human and THOR FEM response data was filtered with CFC 108 4 pole phaseless digital filter that showed effectiveness in reducing the data noise without changing the overall shape of the time histories. Additionally, to reduce excessive noise caused by interaction between the chest accelerometer and non-rigid chest parts, a CFC 60 4-pole phaseless digital filter was applied to the time history of chest acceleration. All filters used were to the specifications outlined in SAE J211 (SAE, 1995).

The THOR-simulation data were compared to human-volunteer data using both the CORA-rating system as well as a biofidelity rating based on ISO 9790. To perform the CORA evaluation, elliptical test corridors (Untaroiu and Lu, 2013) were developed for the acceleration responses of chest and head. The characteristic average curve from each instrumented region was used in the base CORA analysis while the 1 SD (standard deviation) elliptic corridors were used in the CORA biofidelity rating. The ISO 9790 biofidelity score is calculated based on the model-response time-history relative to a test corridor developed from the human-volunteer data (Fig. 11). If the curve is completely within the assigned corridor it receives a score of 10. If the response falls outside the assigned corridor but is within the outer corridor, defined as twice the width of the assigned corridor, the response receives a score of

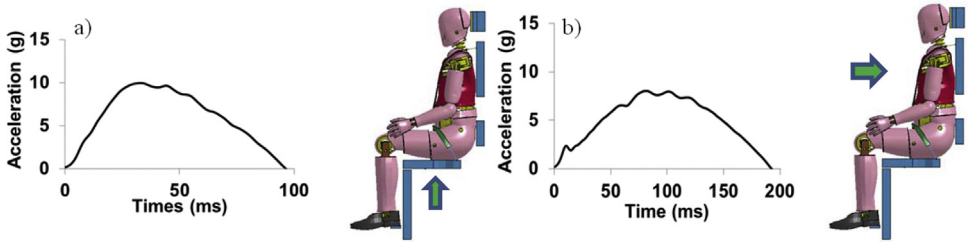

Fig. 9. Model validation: acceleration pulses used in the THOR FEM simulations. (a) Spinal (vertical) direction, (b) frontal (horizontal) direction.

Table 1
The age and anthropometric information of WPAFB male volunteer subjects.

Test	Frontal test: #200301			Spinal test: #199906		
Pulse	6-*g*	8-*g*	10-*g*	6-*g*	8-*g*	10-*g*
# of subjects	55	46	21	25	22	76
Age	30.8 ± 4.7	30.5 ± 4.5	31.7 ± 4.7	31.7 ± 6.3	32.5 ± 6.9	32.5 ± 3.6
Height (mm)	180.0 ± 17.0	182.0 ± 5.5	182.0 ± 5.3	180.0 ± 6.7	182.0 ± 6.6	181.0 ± 6.9
Weight (kg)	89.6 ± 17.2	88.6 ± 18.3	90.9 ± 17.0	86.7 ± 13.1	91.8 ± 13.1	86.6 ± 15.0

g: gravitational acceleration.

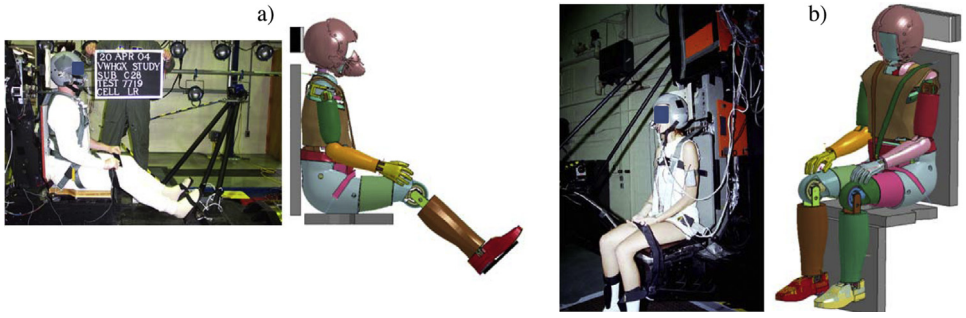

Fig. 10. Human-volunteer test versus FEM: (a) frontal test setup (test #200301) and (b) spinal test setup (test #199906).

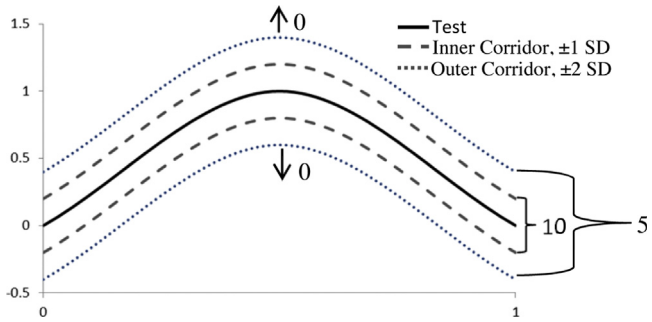

Fig. 11. Example ISO 9790 biofidelity rating corridor.

5. Curves that pass outside the outer corridor receive a score of 0. The total biofidelity score is calculated as the average of all response signal scores, and values greater than 2.6 are considered acceptable for human analysis (Thunert, 2012). Though the test conditions evaluated in this study do not reflect the specific ISO 9790 test regimen, the rating system is used to provide an approximate biofidelity evaluation that encompasses the variation in human test data.

Table 2
Pelvis flesh quasi-static stiffness.

Variable	Original values	Optimized values
Pelvis loading quasi-static scale factor	1.0	0.11

3. Results

3.1. Pelvic flesh calibration under quasi-static loading

The original pelvis-part-material model (approximated based on the material properties defined in the previous THOR FEM), showed a higher stiffness under quasi-static compression loading than the THOR ATD part (Fig. 12a). The optimal scale factor found for the quasi-static stress–strain curve was 0.11 (Table 2). Comparing the pelvic model quasi-static stress–strain curve before and after calibration to generic foam testing gives an approximate Young's modulus of 108 KPa and 12.2 KPa compared to 37.0 KPa (Moore et al., 2007).

By scaling down the stress values in the quasi-static stress–strain curve, the pelvic model closely predicts the response of the physical part during the loading phase (Fig. 12b).

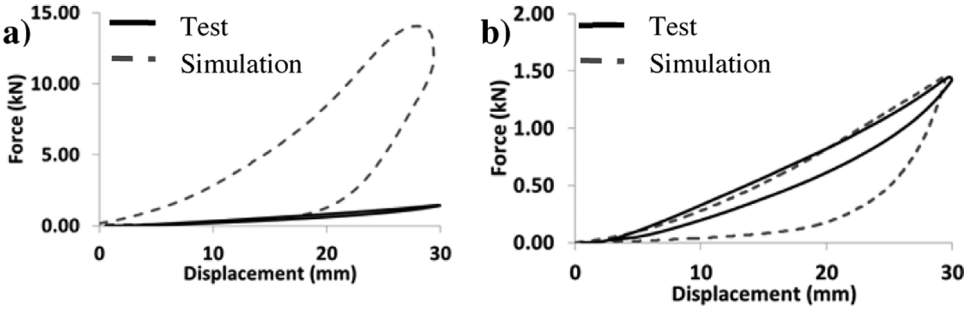

Fig. 12. Pelvis-flesh quasi-static force versus displacement response: (a) pre-optimization, (b) post optimization.

Table 3
The parameters of calibrated material models.

Part	Variable	Original values	Optimized values
UFJ	Loading SF	0.40	0.83
	Unloading SF	0.40	0.22
LFJ	Loading SF	0.40	7.3
	Unloading SF	0.40	9.3
Pelvis	Loading SF1	1.0	0.40
	Loading SF2	1.0	0.57
	Loading SF3	1.0	0.71
	Loading SF4	1.0	0.96
	Shape parameter (SH)	3.0	3.0
	Hysteretic unloading factor (HU)	0.10	0.53

3.2. Calibration of THOR FEM

The UFJ calibration resulted in an increased loading stiffness with decreased unloading stiffness (Table 3). The LFJ stiffness increased dramatically in both loading and unloading. The calibration of the dynamic stiffness curves of the pelvis-flesh-material model resulted in a gradual decrease in stiffness with decreasing strain rate. The energy dissipation was increased in pelvis unloading with increased hysteretic unloading factor and unchanged shape value.

During spinal loading, an improved overall response was observed in the calibrated model. The CORA rating of the FEM increased from 0.75 to 0.93 (out of 1.0) during the calibration process (Fig. 13). The kinematic predictions of the calibrated FEM are very similar to the ATD as shown by the CORA scores of head, thorax, and pelvis acceleration that were above 0.93 (out of 1.0). Significant improvements were observed in the calibrated FEM kinetics as well. The average CORA-rating scores of neck and lumbar forces increased from under 0.72 to above 0.91 (out of 1.0).

An improvement of the calibrated FEM response in frontal loading was observed as well. However, the overall CORA-model rating increased only slightly from 0.69 to 0.73 (out of 1.0) during the calibration process (Fig. 14). While the majority of ATD responses were improved in the calibrated FEM (5 of 7 signals), the pelvis acceleration and lower-neck force response ratings did not. Oscillations in pelvis *x*-acceleration and the continuous increase of the lower-neck *z*-force continued to be predicted by the model but were not observed in testing.

3.3. Validation of the THOR FEM

The calibrated THOR FEM closely predicted ATD response under an independent spinal loading case, receiving an overall CORA rating of 0.85 (out of 1.0) (Fig. 15). As in the calibration, there are some slight differences in neck kinetics between FEM simulations and test data. The upper-neck unloading rate is slightly lower than the test data. Otherwise, the ATD response-time history is predicted by the FEM in all instrumented areas.

During validation, the THOR FEM reasonably predicted the response of the ATD in an independent frontal-loading-test case (Fig. 16). The FEM response received a total CORA score of 0.68 (out of 1.0). As in calibration, the horizontal-pelvis acceleration and lower-neck force predicted by the FEM showed the same trends (not observed in testing) and consequently resulted in the lowest CORA scores (around 0.50).

3.4. Comparison to human responses

3.4.1. Spinal loading

When comparing the THOR responses to human responses in spinal loading, the acceleration response of the THOR FEM generally falls within the range of human response in each spinal impact test condition evaluated (Fig. 17). Head acceleration unloads faster in the THOR FEM than average human response, in the 8-*g* and 10-*g* pulse tests. A total average CORA score of 0.77 (out of 1.0) was achieved over all 3 impact conditions, indicating a reasonable prediction of average human-volunteer response. In addition, the total biofidelity rating of 4.2 (out of 10) indicates an acceptable rating for use in predicting human response in these test conditions.

3.4.2. Frontal loading

For frontal loading, a lower-response correlation between THOR FEM data and human-volunteer-test data is observed in the frontal impact direction compared to the spinal impact direction (Fig. 18). Over all 3 impacts, there is a delay in the THOR FEM head acceleration compared to the characteristic human response; this difference decreases slightly with increasing pulse acceleration. The total average CORA score calculated relative to the average

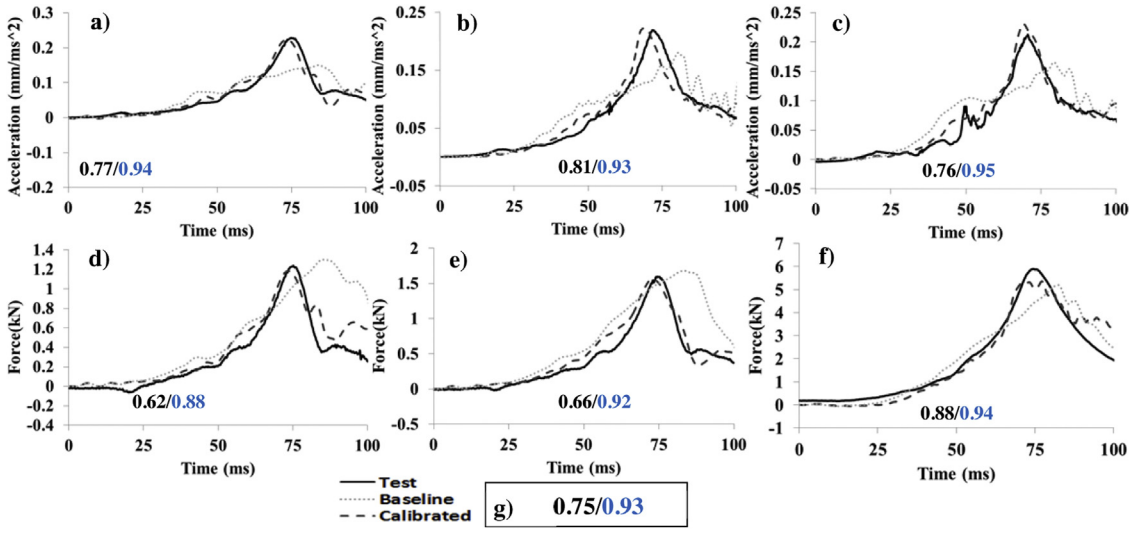

Fig. 13. Model spinal calibration—pulse 10-*g* @ 70 ms impact time-history comparison under spinal loading: (a) head CG *z*-acceleration, (b) thorax CG *z*-acceleration, (c) pelvis *z*-acceleration, (d) upper-neck *z*-force, (e) lower-neck *z*-force, (f) lumbar-spine *z*-force, (g) total CORA rating.

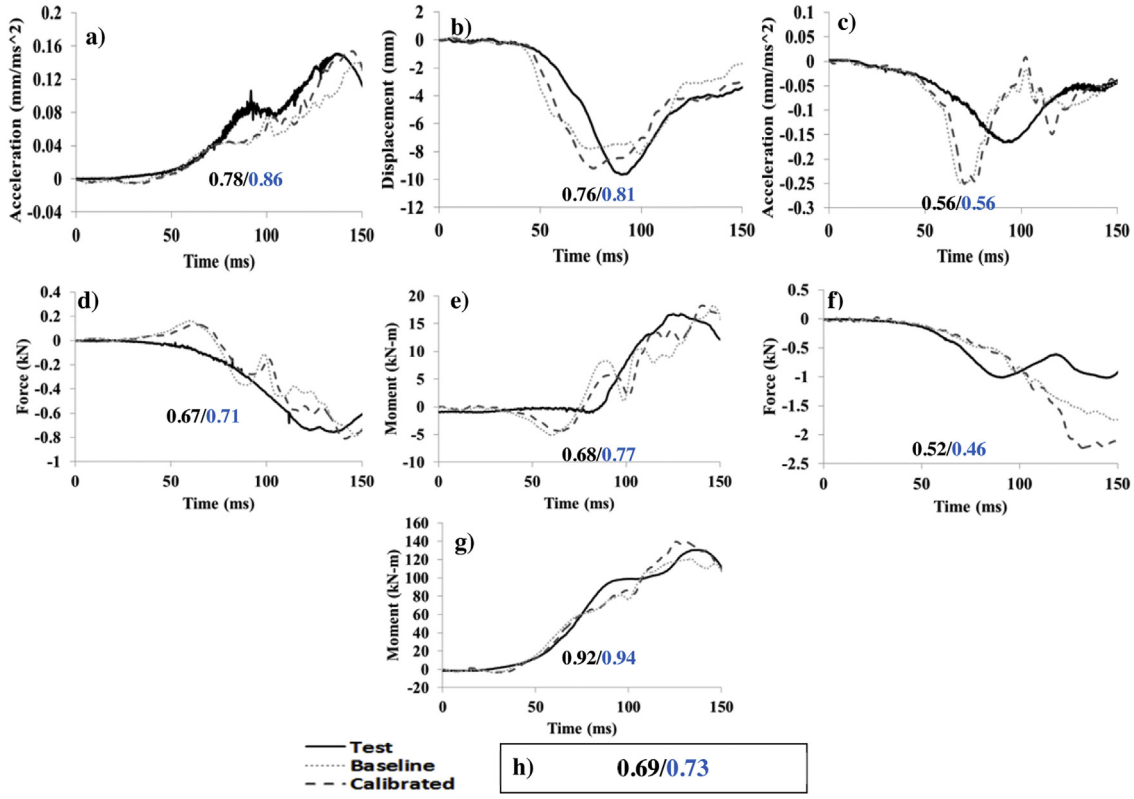

Fig. 14. Model frontal calibration—pulse 10-*g* @ 70 ms impact time-history comparison under frontal loading: (a) head CG *x*-acceleration, (b) chest *x*-displacement, (c) pelvis *x*-acceleration, (d) upper-neck *z*-force, (e) upper-neck *y*-moment, (f) lower-neck *z*-force, (g) lower-neck *y*-moment, (h) total CORA rating.

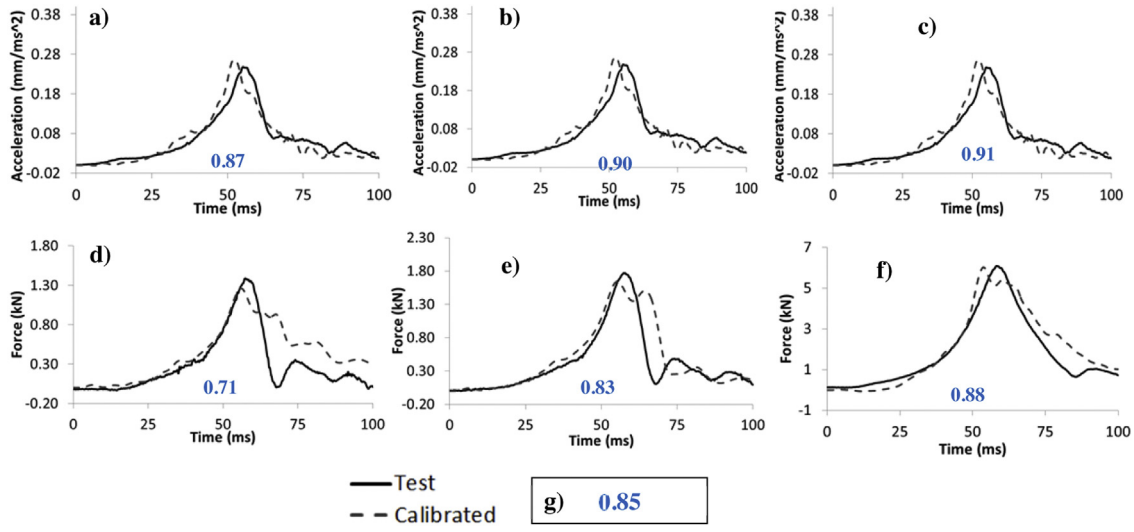

Fig. 15. Model spinal validation—pulse 10-*g* @ 40 ms impact time history comparison under spinal loading: (a) head CG *z*-acceleration, (b) thorax CG *z*-acceleration, (c) pelvis *z*-acceleration, (d) upper-neck *z*-force, (e) lower-neck *z*-force, (f) lumbar-spine *z*-force, (g) total CORA rating.

human frontal impact responses was 0.57 (out of 1.0). The overall chest acceleration time history exhibits a similar shape compared to the test data, although the response is much noisier. After initial peak response, both THOR FEM head and chest exhibit spikes not observed in human response. The total biofidelity rating is 2.5 (out of 10), just under the score for an acceptable prediction of human like response.

4. Discussion

In the field of spaceflight occupant protection it is essential to acquire a test device that accurately mimics human response under impact conditions that crewmembers typically may be subjected. The 50th percentile THOR ATD was chosen by a team of experts as the primary ATD to be evaluated for new NASA

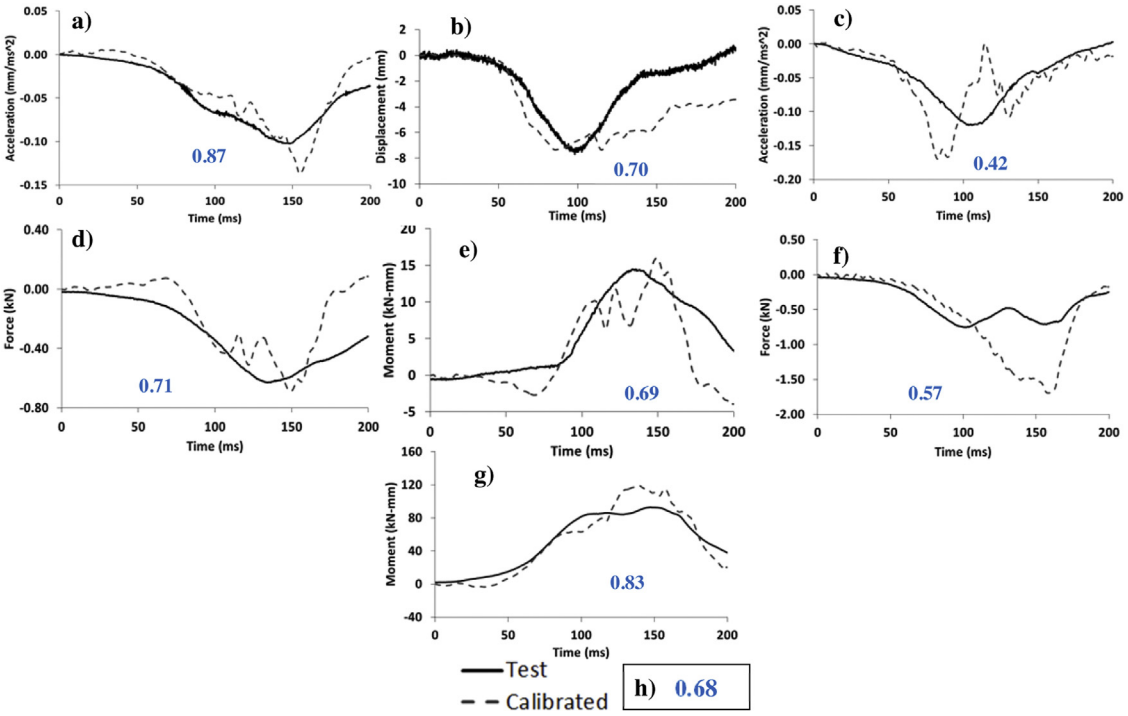

Fig. 16. Model frontal validation—pulse 8-*g* @ 100 ms impact time history comparison under frontal loading: (a) head CG *x*-acceleration, (b) chest *x*-displacement, (c) pelvis *x*-acceleration, (d) upper-neck *z*-force, (e) upper-neck *y*-moment, (f) lower-neck *z*-force, (g) lower-neck *y*-moment, (h) total CORA rating.

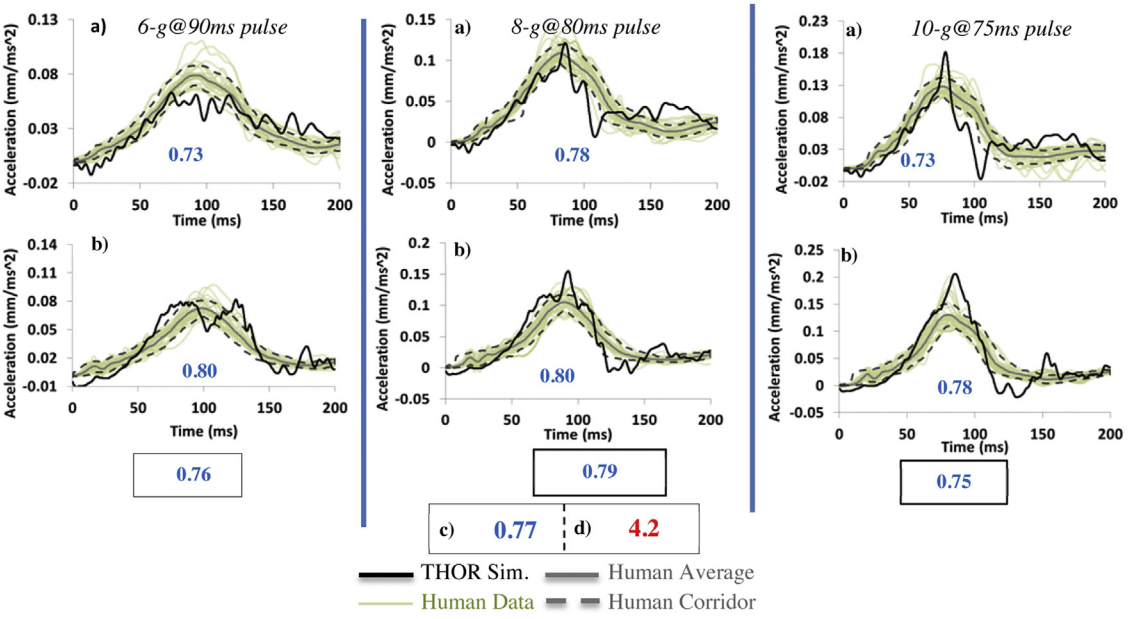

Fig. 17. THOR FEM versus human-volunteer comparison: kinematic responses under spinal loading: (a) head *z*-acceleration, (b) chest *z*-acceleration, (c) total CORA rating, (d) total biofidelity rating.

standards and requirements (Somers et al., 2014b). In the current study, a FEM was developed, calibrated, and validated to reasonably predict the response of the THOR ATD in complex impact events. Previous work on the THOR FEM has been primarily geared towards automotive crash analysis focused on ATD responses under frontal impact loading (Untaroiu et al., 2009; Putnam et al., 2014). In this study for the first time, key components to the THOR FEM response in both spinal and horizontal impacts were identified and calibrated to predict ATD response under loads characteristic of spaceflight impacts. Calibration was performed using a unique optimization protocol based on quantitative comparisons of simulation response to test-time-history data. The time-history signals used in the calibration process were carefully chosen to evenly calibrate the full spectrum of ATD kinetic and kinematic responses (head, thorax, and pelvis regions).

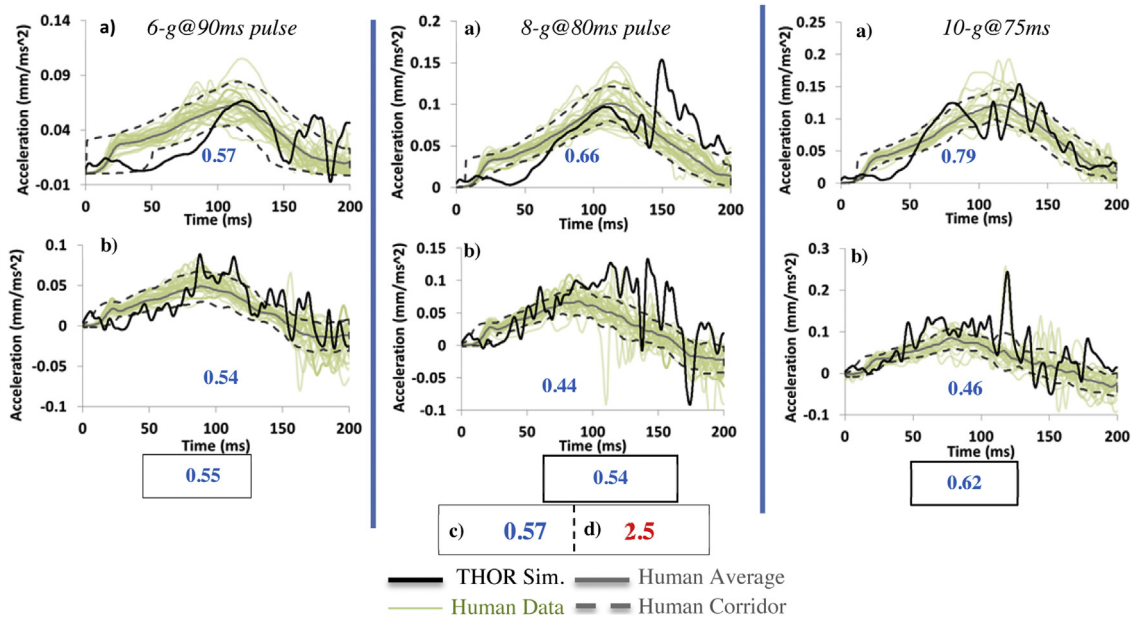

Fig. 18. THOR FEM versus human-volunteer comparison: kinematic responses under frontal loading: (a) head *x*-acceleration, (b) chest *x*-acceleration, (c) total CORA rating, (d) total biofidelity rating.

4.1. THOR FEM calibration and validation

The THOR FEM calibration resulted in large changes to the stiffness characteristics of the material models corresponding to the lumbar joints and pelvis flesh. A decreased stiffness in the pelvis paired with an increased stiffness in the spinal column led to a more accurate transfer of energy through the THOR FEM along the spinal direction. This resulted in a sharper acceleration response throughout the FEM, better predicting the THOR ATD kinematics. In addition, the response shape of the neck and lumbar spine loading were improved.

The material-model calibration improved the predicted shapes of head acceleration and chest deflection by stiffening the head response and allowing for greater chest deflection. However, the most significant model discrepancies were not improved with the updated material models. The change in pelvis stiffness had little effect on pelvis acceleration in the frontal impact cases therefore other possible mechanisms for model discrepancy such as the contact friction defined between seat and model should be further examined. Although the calibration improved the upper neck loading, no improvements were observed in the lower neck loading and pelvis acceleration. While the head-neck FEM was previously calibrated and validated in extension, flexion, and lateral loading (Putnam et al., 2014), the source of these discrepancies could be caused by possible inaccuracies in the thorax model or in the interaction between thorax and restraint system that influence the responses of surrounding regions (neck and pelvis). A further review of this region is suggested. The optimization algorithms used in calibration showed good capability to improve the overall model response. This global approach may reduce the prediction capability in some regions (e.g., lower-neck force during frontal test). Therefore including component simulations corresponding to various FEM body regions in the whole FEM calibration is suggested in the future. While this approach may increase the computational effort, it will help to better debug the possible causes of response discrepancies and improve the FEM response in all loading directions.

4.2. Biofidelity analysis

The comparison of the THOR FEM and human volunteers under spinal loading demonstrated biofidelity of the THOR in terms of the head and chest acceleration. Though one difference that is observed is head acceleration predicted by the FEM was shown to fall more rapidly after peak response than human as the test acceleration pulse decreased. As this was not observed as clearly in the chest, this may be an indication of a stiffer unloading response in the upper spine/neck region of the FEM.

The frontal impact response of the THOR FEM, compared to the human-volunteer-test data, indicates some inaccuracies in the ATD response under frontal loading. Head acceleration predicted by the THOR FEM exhibits an initial lag compared to the human test data, with this lag increasing with increasing input pulse magnitude. After this lag, FEM head acceleration does rise quickly to decently approximate the point of average peak human acceleration. While the THOR FEM approximated relatively well the physical ATD in these regions under frontal loading, the FEM versus human-volunteer differences observed in frontal impact indicate biofidelity limitations of THOR in this impact condition. The delayed peak acceleration present in the head acceleration is an indication of a slower transfer of energy through the upper spine and neck region, compared to human response. This may be due to the upper spine region being too soft in tension. The THOR modification reduced the neck stiffness to better match post mortem human subject (PMHS) test data (Ridella and Parent, 2011) and the FEM head neck model was calibrated to this response (Putnam et al., 2014). The PMHS testing does not account for the resting muscle tone and possible active bracing in human volunteers (Beeman et al., 2012) that would lead to a stiffer neck response, possibly explaining the softer initial response of the THOR FEM compared to the active human volunteers. Thorax differences between the THOR and human volunteer may also play a role in the differences observed in frontal loading. Although, general thorax acceleration response is similar, there also exists a slight delay in response at the onset of the impact. Initial PMHS corridors of thoracic force-

deflection for ATD certification were generated using a hub-impact test condition (Kroell and Schneider, 1971; Lobdell et al., 1973). It has been shown that the thoracic mechanical response depends strongly on the load distribution (Kent et al., 2004), geometrical characteristics of the ribcage, and biological material properties (Gayzik et al., 2008). Difference in thorax biofidelity may be explained by the different thorax loading in the examined condition due to belt loading, compared to the hub-impact tests used in biofidelic certification. These possible limitations should be examined further in future development of the THOR ATD to improve its biofidelity in this condition.

Overall the THOR FEM developed in this study has shown to effectively predict ATD responses in both spinal and frontal loading; however, in frontal loading a few regions could use further improvement. With this known, the FEM can be used as an effective tool for performing crew-impact-safety analysis of future spacecraft in their typical loading environments. In addition, the THOR FEM has been used to demonstrate the ATD's biofidelity in spinal loading, as it closely matched average human response and demonstrated acceptable biofidelity within the range of human variability. Differences observed between THOR and human response in the frontal impact direction may be used to improve upon its design in the future to increase its effectiveness as a tool to predict human injury in these conditions. In the future, human FEMs (Danelson et al., 2011; Thompson et al., 2011) may be used in conjunction with the developed THOR FEM to develop new injury criteria specific to spaceflight loading conditions.

5. Conclusions

In this study a calibration protocol was developed and implemented to improve the accuracy of the THOR FEM in specific spaceflight loading conditions. This calibration protocol has been shown to be effective, as the prediction of ATD responses in examined testing conditions were improved. Furthermore, validation simulations proved the robustness of the final model effectiveness as well as the calibration process used. However, to achieve complete model confidence, extensive validation at various loading conditions should be performed when test data becomes available.

Once calibrated to the spaceflight testing conditions, the developed THOR FEM provided an effective tool to evaluate ATD biofidelity in spaceflight conditions against historic human volunteer test data. The THOR FEM closely predicted human-volunteer response in spinal loading in a variety of acceleration conditions, indicating biofidelity of the ATD along this loading direction. The THOR FEM exhibited a softer response than human-volunteers in the frontal impact testing conditions. Based on these results, improvements to the material and structural components of the THOR ATD and FEM are suggested.

Acknowledgments

This work was funded by the NASA Human Research Program through the Bioastronautics Contract (NAS9-02078). The authors would also like to thank Toyota Motor Corporation (Japan) for meshing the updated pelvis FEM, and NHTSA(USA) for providing the THOR ATD for testing and the pelvic test data. All findings and views reported in this manuscript are based on the opinions of the authors and do not necessarily represent the consensus or views of the funding organization.

References

Adam, T., Untaroiu, C.D., 2011. Identification of occupant posture using a Bayesian classification methodology to reduce the risk of injury in a collision. Transp. Res. Part C Emerg. Technol. 19 (6), 1078–1094.
Beeman, S.M., Kemper, A.R., Madigan, M.L., Franck, C.T., Loftus, S.C., 2012. Occupant kinematics in low-speed frontal sled tests: human volunteers, hybrid III ATD, and PMHS. Accid. Anal. Prev. 47, 128–139.
Bose, D., Crandall, J.R., Untaroiu, C.D., Maslen, E.H., 2010. Influence of pre-collision occupant parameters on injury outcome in a frontal collision. Accid. Anal. Prev. 42 (4), 1398–1407.
Buhrman, J., 1998. The AFRL Biodynamics Data Bank and Modeling Applications. Dayton, OH.
Cheng, H., Buhrman, J., 2000. Development of the afrl biodynamics data bank and web user interface. In: Sae (Ed.), SAE Technical Paper 2000-01-0162. SAE (Society of Automotive Engineers), Detroit, MI.
Danelson, K.A., Bolte, J.H., Stitzel, J.D., 2011. Assessing astronaut injury potential from suit connectors using a human body finite element model aviation. Space Environ. Med. 82 (2), 79–86.
Foust, J., 2014. NASA selects Boeing and SpaceX for commercial crew contracts. http://spacenews.com/41891nasa-selects-boeing-and-spacex-for-commercial-crew-contracts/.
Gayzik, F.S., Yin, M., Danelson, K., Slice, D., Stitzel, J., 2008. Quantification of age-related shape change of the human rib cage through geometric morphometrics. J. Biomech. 41 (7), 1545–1554.
Gehre, C., Gades, H., Wernicke, P., 2009. Objective rating of signals using test and simulation responses. ESV Conference, Stuttgart, Germany.
Jacob, C., Charras, F., Trosseille, X., Hamon, J., Pajon, M., Lecoz, J.Y., 2000. Mathematical models integral rating. Int. J. Crashworthiness 5 (4), 417–432.
Kent, R., Lessley, D., Sherwood, C., 2004. Thoracic response to dynamic, non-impact loading from a hub, distributed belt, diagonal belt, and double diagonal belts. Stapp Car Crash J. 48, 495.
Kroell, C.K., Schneider, D.C., 1971. Impact tolerance and response of the human thorax biomechanics of impact injury and injury tolerances of the thorax–shoulder complex. Proceedings of the 15th Stapp Car Crash Conference .
Lobdell, T.E., Kroell, C.K., Schneider, D.C., Hering, W.E., Nahum, A.M., 1973. Impact response of the human thorax. In: King, W., Mertz, H. (Eds.), Human Impact Response. Springer, US, pp. 201–245.
LS-DYNA, 2007. Keyword User's Manual. LSTC.
Mike Beebe, P.D., 2010. THOR-NT Pelvis, Femur, Knee Revisions. NHTSA.
Moore, B., Jaglinski, T., Stone, D., Lakes, R., 2007. On the bulk modulus of open cell foams. Cell. Polym. 26 (1), 1–10.
Newby, N., Somers, J.T., Caldwell, E.E., Perry, C., Littell, J., Gernhardt, M., 2013. Assessing biofidelity of the test device for human occupant restraint (THOR) against historic human volunteer data. Stapp Car Crash J. 57, 469–505.
NHTSA, 2014. 2013 Motor Vehicle Crashes: Overview, Report nr. DOT HS 812 101, website: http://www-nrd.nhtsa.dot.gov/Pubs/812101.pdf.
Pellettiere, J., Moorcroft, D., 2012. Occupant calibration and validation methods. In: Duffy, V.G. (Ed.), Advances in Applied Human Modeling and Simulation. CRC Press, Boca Raton, FL, pp. 307–316.
Putnam, J.B., Somers, J.T., Untaroiu, C.D., 2014. Development, calibration, and validation of a head–neck complex of THOR mod kit finite element model. Traffic Inj. Prev. 15 (8), 844–854.
Putnam, J.B., Untaroiu, C.D., Littell, J., 2015. Finite element model of the THOR-NT dummy under vertical impact loading for aerospace injury prediction: Model evaluation and sensitivity analysis. J. Am. Helicopter Soc. 60 (2), 1–10.
Putnam, J.B., Untaroiu, C.D., Littell, J., Annett, M., 2013. Validation and sensitivity analysis of a finite element model of THOR-NT ATD for injury prediction under vertical impact loading. Proceedings of the AHS International 69th Annual Forum, Phoenix, AZ, USA, pp. 38–47.
Ridella, S.A., Parent, D.P., 2011. Modifications to improve the durability, usability and biofidelity of the THOR-NT dummy. The 22nd ESV Conference, Washington, D.C., USA.
SAE, 1995. Instrumentation for impact test–part 1: electronic instrumentation. SAE paper no. J211/1. Society of Automotive Engineers, Warrendale, PA.
Sarin, H., Kokkolaras, M., Hulbert, G., Papalambros, P., Barbat, S., Yang, R.J., 2008. A comprehensive metric for comparing time histories in validation of simulation models with emphasis on vehicle safety applications. ASME International Design Engineering Technical Conference and Computers and Information in Engineering Conference (DETC' 08), New York, USA.
Shaw, G., Crandall, J., Butcher, J., 2002. Comparative evaluation of the THOR advanced frontal crash test dummy. Int. J. Crashworthiness 7 (3), 239–253.
Somers, J.T., Caldwell, E., Newby, N., Maher, J., Gernhardt, M., Untaroiu, C., Putnam, J., 2014a. Test device for human occupant restraint (THOR) multi-directional biodynamic response testing. NASA .
Somers, J.T., Newby, N., Lawrence, C., DeWeese, R., Moorcroft, D., Phelps, S., 2014b. Investigation of the THOR anthropomorphic test device for predicting occupant injuries during spacecraft launch abort and landing. Front. Bioeng. Biotechnol. doi:http://dx.doi.org/10.3389/fbioe.2014.00004 2,4.
Strzelecki, J.P., 2005. Characterization of horizontal impulse accelerator pin profiles Report nr. AFRL-HE-WP-SR-2006-0057.
Thompson, A., Gayzik, F., Moreno, D., Rhyne, A., Vavalle, N., Stitzel, J., 2011. A paradigm for human body finite element model integration from a set of regional models. Biomed. Sci. Instrum. 48, 423–430.

Thunert, C., 2012. Cora Release 3.6, User's Manual. PDB.
Untaroiu, C., Lim, J., Shin, J., Crandall, J., Malone, D.P., Tannous, R.E., 2009. Evaluation of a finite element of the THOR-NT dummy in frontal crash environment. ESV Conference, Stuttgart, Germany.
Untaroiu, C.D., Lu, Y.C., 2013. Material characterization of liver parenchyma using specimen-specific finite element models. J. Mech. Behav. Biomed. Mater. 26, 11–22.
Untaroiu, C.D., Shin, J., Crandall, J.R., 2007. A design optimization approach of vehicle hood for pedestrian protection. Int. J. Crashworthiness 12 (6), 581–589.
Untaroiu, C.D., Shin, J., Lu, Y.C., 2013. Assessment of a dummy model in crash simulations using rating methods. Int. J. Automot. Technol. 14 (3), 395–405.
Yue, N., Shin, J., Panzer, M.B., Crandall, J., Parent, D.P., 2013. Updates of the lower extremity of THOR-NT 50th finite element dummy to mod kit specification. The 23rd ESV Conference, Seoul, Korea.